14th Australasian Fluid Mechanics Conference
Adelaide University, Adelaide, Australia
10-14 December 2001

Analysis of Four Data Reduction Schemes Applied to Four-sensor Hot-wire Probes

P. Lavoie and A. Pollard

Department of Mechanical Engineering
Queen's University, Kingston, Ontario, K7L 3N6 CANADA

Abstract

Four data reduction schemes for four-sensor hot-wire probes have been implemented and used to measure the turbulent statistics in the near field of a round jet. Each data reduction scheme was used on the set of signals obtained and compared to data from the literature and LES computation to quantify the level of accuracy of the probe and the data reduction schemes proposed in the literature in a consistent manner. Results for u'_{rms}, $u'v'$ and $v'w'$ are presented.

Introduction

Hot-wire probes with more than two wires have been developed to measure simultaneously all three components of velocity. Simultaneous measurement of three velocity components improves the accuracy of measurements in highly turbulent, three-dimensional flows and can reduce the time required to acquire data when compared to the use of traditional single and X-wire probes. Various four wire probe geometries have been described in the literature and are usually preferred over three-wire probes due to their slightly larger acceptance domain and increased accuracy [7]. These improvements can be attributed to the fourth, "redundant" wire that can provide additional information about the flow. Four-sensor hot-wire probes like the one used for this study have become available commercially.

The reduction of the four signals into a three-dimensional velocity vector becomes an over-determined, nonlinear system when four sensors are used to measure the three components of velocity. This complicates data analysis compared to traditional hot-wire probes. A variety of data reduction schemes, based on analytical equations and/or look-up tables, have been developed over the years to tackle these complications [2, 4, 8, 7, 13]. Some methods solve the system of equations using a least-square approach, while others form a system of three equations that can be solved directly, based on either analytical or empirical functions. Depending on the way the signals are used to extract the velocity vector and on the assumptions made, each data reduction scheme will have different characteristics regarding the size of the acceptance domain and the accuracy of the results.

In this paper, a consistency of approach (i.e. same data, same experimental rig, same filter and bridge settings, and same experimenter) is used to quantify the level of accuracy of the probe and the data reduction schemes that have been proposed in the literature. The four data reduction schemes are used to reduce measurements taken in the near field of a round jet, the results of which are compared to each other, data from the literature and LES computations.

Calibration Rig and Procedure

A novel calibration rig has been designed for *in situ* calibration of the probe. The rig consists of a round jet with a diameter of 6.35 cm with a variable velocity axial fan capable of producing velocities between 1 m/s and 22 m/s at the jet exit. The shape of the converging nozzle is defined by a fifth order polynomial to provide a flat velocity profile at the exit plane (profile constant to $\pm 0.5\%$). The jet is mounted on gimbals to allow rotation in yaw(α) and pitch(β) relative to the center point of the exit plane. Two stepper motors enable rotation of the jet with respect to the fixed probe within a cone angle of $\pm 35^o$ in both α and β. A Pitot-static tube is attached onto the nozzle and oriented parallel to the flow to measure the exit velocity.

For a typical calibration, α and β are varied in steps of 5^o within a circle of 70^o in diameter for a total of 184 angular positions. For each position, 12 velocity levels are measured in the range of 6 to 22 m/s. LabVIEW is used to automate the calibration and data acquisition procedures, which takes about 5 hours. If the directional response of the probe is uncoupled from the velocity magnitude (see below), the effective velocity calibration consists of 20 velocity points taken between 2 and 22 m/s with the probe aligned with the flow.

The Four-sensor Probe and Experimental Setup

An AUSPEX AVEP-4-103 four-sensor hot-wire is used (see figure 1). Four 5 μm tungsten wires with a length of 1 mm are placed in a square-base pyramid. The sensor wires are oriented at 45^o to the probe and 90^o from each other. To avoid cross-talk between the wires, there is no common central prong.

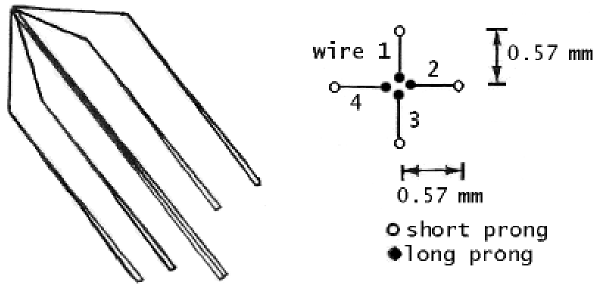

Figure 1: Four-sensor probe geometry

The free jet facilities consist of a variable velocity centrifugal fan, which provides the air flow to a converging nozzle with an exit diameter of 7.2 cm. The signals from the probe were sampled at 14 kHz for 15 seconds for each data point. Experiments were done at a Reynolds number of approximately 74,000. A thermocouple was used to measure the air temperature and the signals were corrected for temperature changes with the linear correction formula [1].

The Data Reduction Schemes

The four data reduction schemes used in this study will be briefly described in this section, more details are provided in the original papers. For the purpose of this paper, each method will be referred to by the name of the first author of the paper that introduced the technique.

The first method considered is by Marasli *et al.* [8]. This method depends entirely on analytical equations to relate the probe signals to the velocity vector. The equation relates the output signal from one of the wires to an effective cooling velocity. Although King's Law has been traditionally used for this, a fourth order polynomial is used in this case.

$$U_{eff,i}^2 = a_0 + a_1 e + a_2 e^2 + a_3 e^3 + a_4 e^4 \tag{1}$$

where e is the voltage output from the sensor and the subscript 'i' is an integer between 1 and 4 that represents each of the sensors.

Jorgensen's directional response equation [5] is used to relate $U_{eff,i}$ to the three-dimensional velocity vector sensed by each wire.

$$U_{eff,i}^2 = u_N^2 + k^2 u_T^2 + h^2 u_B^2 \tag{2}$$

where u_N, u_T and u_B are the normal, tangential and bi-normal components of the velocity with respect to the sensor respectively, while k and h are the tangential and bi-normal cooling coefficients respectively. It is more convenient to express Jorgensen's equation in terms of u, v and w, the velocity components in the global coordinate system, as follows

$$U_{eff,i}^2 = b_0 u^2 + b_1 v^2 + b_2 w^2 + b_3 uv + b_4 uw + b_5 vw \tag{3}$$

where the b_j coefficients are functions of k, h and the orientation of the sensor relative to the global coordinate system. Since the geometry and thermal coefficients are combined, they can be determined together by direct calibration and hence the exact orientation of each individual sensor does not need to be known. If equations 1 and 3 are combined and then divided by b_0 to make the u^2 coefficient unity, one obtains

$$u^2 - K_{1,i} v^2 - K_{2,i} w^2 - K_{3,i} uv - K_{4,i} uw - K_{5,i} vw = P_i(e), \tag{4}$$

where

$$P_i(e) = A_{0,i} + A_{1,i} e + A_{2,i} e^2 + A_{3,i} e^3 + A_{4,i} e^4 \tag{5}$$

The parameters of equations 4 and 5 are solved simultaneously using a least-square method.

It is important here to note that the k and h parameters have been assumed constant over the full angular and velocity range. Marasli *et al.* warn that this assumption is not valid for yaw and pitch angles in excess of $\pm 20^o$. The calibration range for the present study is $\pm 35^o$. This method is in fact used here as a benchmark to quantify the improvements introduced by look-up tables, which take into account changes in k and h at large angles of attack.

In order to determine the instantaneous velocity vector, the right hand and left hand sides of equation 4 are compared to form a residual equation for each sensor

$$f_i \equiv u^2 - K_{1,i} v^2 - K_{2,i} w^2 - K_{3,i} uv - K_{4,i} uw - K_{5,i} vw - P_i(e) \tag{6}$$

The velocity vector is then taken as the vector that minimizes the residual defined by

$$F = \sum_{i=1}^{4} f_i^2 \tag{7}$$

Newton's method is used to minimize F. An initial guess was obtained by treating the four-sensor probe as two X-wires. See Wygnanski *et al.* [14] for a description of the calibration procedure used.

The next method considered is by Döbbeling *et al.* [4]. This method is the first of three that are based on look-up tables. For this method, the effective cooling velocity concept is used to uncouple the velocity magnitude from the directional response of the probe. An empirical directional function is defined by

$$\begin{aligned} U_{eff,i} &= P_i(e_i) \\ U_{eff,i}^2 &= Q^2 \times g_i(\alpha,\beta) \end{aligned} \tag{8}$$

where P_i is a fourth order polynomial, Q is the velocity magnitude and $g_i(\alpha,\beta)$ is the directional response function.

To determine the velocity vector from the probe signals a residual function is defined by

$$E_{sq} = \sum_{i=1}^{4} \left(\frac{U_{eff,i}^2(e_i)}{\sum_{i=1}^{4} U_{eff,i}^2(e_i)} - \frac{g_i(\alpha,\beta)}{\sum_{i=1}^{4} g_i(\alpha,\beta)} \right)^2 \tag{9}$$

An iterative algorithm is used to minimize E_{sq} and solve for the direction of the velocity vector. Once the direction of the vector is known, its magnitude can be found from a modified version of equation 8.

$$Q = \left(\frac{1}{4} \sum_{i=1}^{4} \frac{U_{eff,i}^2(e_i)}{g_i(\alpha,\beta)} \right)^{\frac{1}{2}} \tag{10}$$

The third technique is from Wittmer *et al.* [13]. The motivation behind this method was to find empirical functions that would have a slow rate of change so that a simple interpolation scheme could be used without the introduction of large errors. To achieve this goal analytical functions are used to make a first, rough estimate of the velocity vector. Three correction functions can then be defined to relate the estimated to the real velocity vectors.

$$\Phi = f_j(V_e/Q_e, W_e/Q_e) \cdot Q_e + \Phi_e \quad j = 1,2,3 \tag{11}$$

where the subscript 'e' marks an estimated value and Φ is replaced by V, W and Q for j=1, 2 and 3, respectively. Note that the estimate for the velocity magnitude is used by this method to uncouple the velocity and directional response functions. See [13] for equations used to estimate velocity vectors.

In the case of Marasli and Döbbeling, the acceptance domain of the probe is larger than the current calibration range, assuming the error levels are acceptable at these large angles of attack. However, for Wittmer it is found that the correction functions can take more than one value for a given $(V_e/Q_e, W_e/Q_e)$. The acceptance domain then needs to be restricted to the range where f_1, f_2 and f_3 are single valued. The edge of this domain can be identified from a change of sign in the Jacobian defined by

$$\frac{\partial(V_e/Q_e, W_e/Q_e)}{\partial(V/Q, W/Q)} \tag{12}$$

The acceptance domain of this method is larger than 35^o in the axis of the sensors but can be as small as 31^o in the region diagonal to those axes (see figure 2).

The last technique studied was developed by Béharelle [2]. For this method, the effective velocity concept is used to uncouple the velocity magnitude to the directional response of the probe. In this case two angular coefficients, K_α and K_β, and one correction coefficient for the velocity magnitude, C_q, are used. These coefficients are defined in terms of velocity independent coefficients, A_i, computed for each wire from the calibration.

$$A_i = < U_{eff,i}(\alpha,\beta) Q > / < QQ > \tag{13}$$

where $< >$ are averages over all velocity levels. Equation 1 is used to express $U_{eff,i}$ as a function of the output signal of the

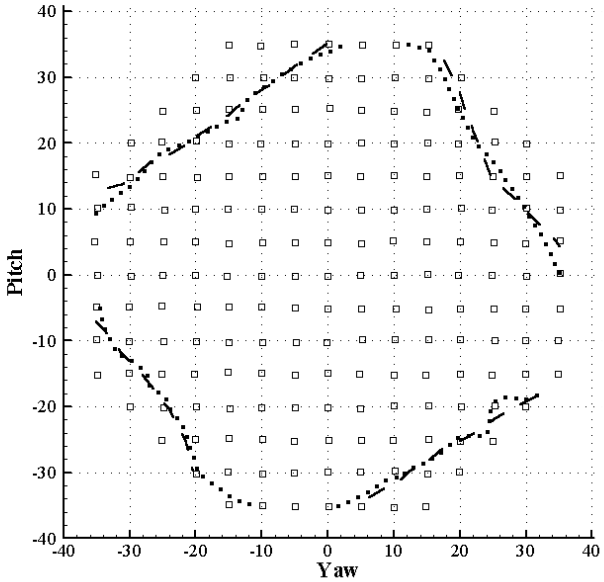

Figure 2: Acceptance domain of Wittmer (dotted line) and Béharelle (dashed line). Each square is one calibration point.

wires. K_α, K_β and Cq are defined as

$$\begin{aligned} K_\alpha(\alpha,\beta) &= (A_4^2 - A_3^2)/(A_4^2 - A_3^2) \\ K_\beta(\alpha,\beta) &= (A_1^2 - A_2^2)/(A_1^2 - A_2^2) \\ C_q(\alpha,\beta) &= (A_1^2 + A_2^2 + A_3^2 + A_4^2)/4 \end{aligned} \tag{14}$$

For easy data reduction, the functions K_α and K_β can be inverted to give the yaw and pitch angles, α and β, as a function of K_α and K_β. These two parameters can be computed from the effective velocity sensed by each wire in the data reduction phase using:

$$\begin{aligned} K_\alpha &= (U_{eff,4}^2 - U_{eff,3}^2)/(U_{eff,4}^2 + U_{eff,3}^2) \\ K_\beta &= (U_{eff,1}^2 - U_{eff,2}^2)/(U_{eff,1}^2 + U_{eff,2}^2) \end{aligned} \tag{15}$$

As in the case of Wittmer's correction functions, regions with more than one possible yaw and pitch combination for a given set of K_α and K_β values are found. The acceptance region of this method is thus restricted to the region where only one solution is possible (see figure 2). The edge of the domain can be found from a change in sign of the Jacobian defined by

$$\frac{\partial(K_\alpha, K_\beta)}{\partial(\alpha,\beta)} \tag{16}$$

Once the direction of the velocity vector is known, the velocity magnitude, Q, can be computed from the correction function C_q

$$Q^2 = \frac{U_{eff,1}^2 + U_{eff,2}^2 + U_{eff,3}^2 + U_{eff,4}^2}{4 \cdot C_q(\alpha,\beta)} \tag{17}$$

It is relevant to discuss the effects of uncoupling velocity magnitude and direction. It is well known that the directional response of a hot-wire, though constant for velocities above 10 m/s, changes at lower velocities [7]. Though it is possible to compute the directional response at multiple velocity levels and include these in the look-up table algorithm, most researchers elect not to do so due to the exponential increase in computational time necessary in the data reduction phase. Though quantification of this issue is outside the scope of this paper, it is important to keep this source of error in mind especially when measurements are made at low velocity. This issue is studied in details by Lavoie [6].

Presentation and Discussion of Results

First, to verify the accuracy of each scheme, the signals from the calibration points were reprocessed by each data reduction scheme. In addition, the calibration rig was used to generate velocity vectors distributed over the acceptance domain of the four schemes. The results of these points as reduced by each method were compared to the known velocity vectors. The results of these two tests are summarized in table 1. It can be seen from table 1 that Béharelle and Wittmer have error levels that are similar over their acceptance domain. Döbbeling displays slightly larger errors; however, it is more accurate than Marasli, which is the least accurate method of the four considered. When the error was plotted as a function of velocity direction for a given velocity magnitude, it was found that Béharelle and Wittmer offer a constant level of accuracy over the full acceptance domain. Döbbeling and Marasli exhibited error peaks in the diagonal axes as high as 10% on velocity magnitude and 14^o on direction.

Figure 3 presents u'_{rms} and figure 4 presents the $u'v'$ and $v'w'$ profiles as measured at $x/D = 3$ of a round jet with the four-wire probe. u'_{rms} is normalized by the centreline velocity U_{cl}, while $u'v'$ and $v'w'$ are normalized by the square of the centerline velocity. The figures include measurements taken by Sami *et al.* [12] and Citriniti [3], and LES computation by McIlwain [10]. Measurements taken with a single hot-wire are included in figure 3. The profiles are given as a function of the radial distance, r, from the center of the jet normalized by the jet diamter, D.

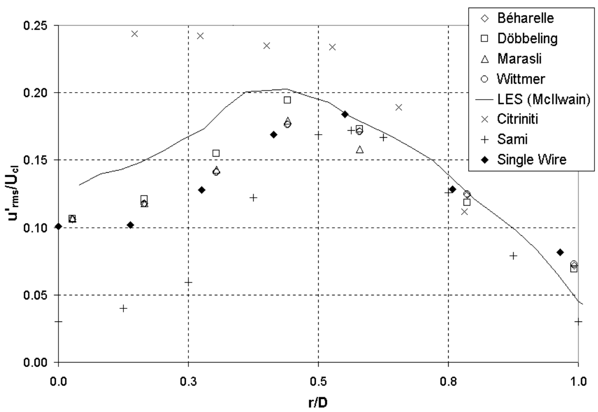

Figure 3: Profile of the RMS of axial fluctuating velocity component, u'.

It can be seen that the profiles measured by the four-wire probe, though similar in shape, are different in magnitude to the experimental data and the simulations obtained from Large Eddy Simulation. However, the similarity between the four-wire and single wire measurements suggests that the differences may be due to non-similar initial conditions of the jet. The experiments by Sami *et al.* [12], for instance, were done at a Reynolds number of 220,000 rather than 74,000 and the LES results, for $Re = 68,000$, axially forced the flow at the preferred frequency to give $St = 0.35$, see Macrouyre *et al* [9]. Olsson and Fuchs [11] found that higher Reynolds number flows will produce smaller fluctuating velocity components which is consistent with the differences between each data set of figures 3 and 4.

u'_{rms} measured by Beharelle and Wittmer are never different by

	Marasli		Döbbeling		Wittmer		Béharelle	
	Velocity	Direction	Velocity	Direction	Velocity	Direction	Velocity	Direction
Group A	1.82%	1.68^o	1.39%	1.10^o	1.22%	0.96^o	1.16%	0.87^o
Group B	1.01%	1.19^o	1.18%	0.98^o	0.90%	0.65^o	0.88%	0.63^o

Table 1: Error on points processed by the four data reduction schemes. Group A: Calibration points within acceptance domain, Group B: Velocity vectors generated with calibration rig.

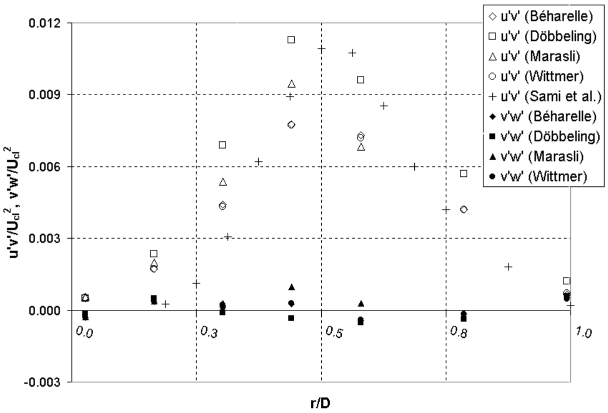

Figure 4: Turbulent shear stress profiles, $u'v'$ and $v'w'$.

more than 1% of the local value, while $u'v'$ is always within 1.6%. Döbbeling and Marasli display larger deviations, up to respectively 10% and 1.5% on u'_{rms}, and deviations of up to respectively 55% and 20% in $u'v'$, when compared to the results of the other two schemes. $v'w'$ should be equal to zero because of circumferential symmetry. Indeed, the normalized value of $v'w'$ as measured by the four-wire probe is typically less $\pm 5 \times 10^{-4}$. The deviation from zero offers a measure of the accuracy of the four-wire probe to measure Reynolds stresses. The results from Béharelle, Wittmer and Marasli match more closely the u'_{rms} measured with the signal wire (typically within 5%), while Döbbeling displays deviation as high as 15%.

Conclusions

The effects of using different data reduction schemes were studied in a systematic manner. Despite the fundamental differences in the techniques proposed by Béharelle and Wittmer, it was shown that these two data reduction procedures provide virtually identical results in the near field of a jet. From calibration results, Béharelle and Wittmer have also exhibited better accuracy than Marasli and Döbbeling, although their acceptance domain was shown to be smaller than those of the former.

Acknowledgements

This work was supported by grants from the Natural Science and Engineering Research Council of Canada.

References

[1] Abdel-Rahman, A., Tropea, C., Slawson, P and Strong, A., On temperature compensation in hot-wire anemometry, *J. Phys. E: Sci. Instrum.*, **20**, 1987, 315-319.

[2] Beharelle, S, Influence du cisaillement transversal sur le développement d'une couche cisaillée libre turbulente incompressible, *PhD Thesis*, Université de Poitiers, 1999.

[3] Citriniti, J. H., Experimental investigation into the dynamics of the axisymmetric mixing layer utilizing the proper orthogonal decomposition, *PhD Thesis*, University of New York at Buffalo, 1996.

[4] Döbbeling, K., Lenze, B. and Leuckel, W., computer-aided calibration and measurements with a quadruple hotwire probe, *Exp. in Fluids*, **8**, 1990, 257–262.

[5] Jorgensen, F.E., Directional sensitivity of wire and fibre film probes, *DISA Info*, **11**, 1971, 31–37.

[6] Lavoie, P., The Accuracy and Validity of Multi-Sensor Hot-Wire Probes and Four Data Reduction Schemes, *MSc Thesis*, Queen's University, 2001.

[7] Maciel, Y. and Gleyzes, C., Survey of multi-wire probe data processing techniques and efficient processing of four-wire probe velocity measurements in turbulent flows, *Exp. in Fluids*, **29**, 2000, 66–78.

[8] Marasli, B., Nguyen, P. and Wallace, J.M., A calibration technique for multiple-sensor hot-wire probes and its application to vorticity measurements in the wake of a circular cylinder, *Exp. in Fluids*, **15**, 1993, 209–218.

[9] Marcouyre, M., McIlwain, S. and Pollard, A., Large eddy simulation of the near field of round jets with vortex-generating tabs, *Proc. of the Second International Symposium on Turbulence and Shear Flow Phenomena, Stockholm*, 2001.

[10] McIlwain, S., Large eddy simulation of the near field of round and coaxial jets with mild swirl, *PhD Thesis*, Queen's University, 2001.

[11] Olsson, M. and Fuchs, L., Large eddy simulation of the proximal region of a spatially developing circular jet, *Physics of Fluids*, **8(8)**, 1996, 2125-2137.

[12] Sami, S., Carmody, T. Rouse, H., Jet diffusion in the region of flow establishment, *J. Fluid Mech.*, **27**, 1967, 231–252.

[13] Wittmer, K.S., Devenport, W.J. and Zsoldos, J.S., A four-sensor hot-wire probe system for three-component velocity measurement, *Exp. in Fluids*, **24**, 1998, 416–423.

[14] Wygnanski, I., Champagne, F. and Marasli, B., On the large-scale structures in two-dimensional, small-deficit, turbulent wakes, *J. Fluid Mech.*, **168**, 1986, 31–71.